

Article

Study on Spatio-Temporal Evolution Law and Driving Mechanism of PM_{2.5} Concentration in Changsha–Zhuzhou–Xiangtan Urban Agglomeration

Wenhao Chen ¹, Chang Zeng ¹, Chuheng Ding ², Yingfang Zhu ³ and Yurong Sun ^{3,*}¹ School of Business, Central South University of Forestry and Technology, Changsha 410004, China² Bangor College China, Central South University of Forestry and Technology, Changsha 410004, China³ College of Science, Central South University of Forestry and Technology, Changsha 410004, China

* Correspondence: yurongsun@csuft.edu.cn; Tel.: +86-130-3733-9678

Abstract: Since the 21st century, China has made many explorations to alleviate the increasingly serious air pollution problem. This study analyses the spatio-temporal evolution characteristics and future development of PM_{2.5} concentration in the Changsha–Zhuzhou–Xiangtan urban agglomeration from 2008 to 2019. In addition, the driving mechanism of spatial differentiation of PM_{2.5} concentration in this urban agglomeration was also investigated. The results were as follows. Firstly, the PM_{2.5} concentration showed a trend of gradual decline between 2008 and 2019. Secondly, the PM_{2.5} concentration distribution was high in the northwest and low in the southeast. Thirdly, PM_{2.5} concentration showed a strong spatial agglomeration. Fourth, except for some rural areas of Chaling County and Yanling County, the concentration of PM_{2.5} in other areas was very likely to continue the past trend of gradual decline. Finally, natural and meteorological conditions played a leading role in the evolution of PM_{2.5} concentration. The influence of socioeconomic factors is small now, but the trend is increasing. To improve air quality deeply, policymakers need to promote comprehensive control of regional air pollution by simultaneously reducing emissions and taking comprehensive treatment. They also need to strengthen supervision to prevent excessive pollution in some rural areas from worsening air quality in the surrounding areas.

Keywords: resource-saving and environment-friendly society; air pollution; Hurst index

Citation: Chen, W.; Zeng, C.; Ding, C.; Zhu, Y.; Sun, Y. Study on Spatio-Temporal Evolution Law and Driving Mechanism of PM_{2.5} Concentration in Changsha–Zhuzhou–Xiangtan Urban Agglomeration. *Sustainability* **2022**, *14*, 14967. <https://doi.org/10.3390/su142214967>

Academic Editors: Weixin Yang, Guanghui Yuan and Yunpeng Yang

Received: 18 August 2022

Accepted: 10 November 2022

Published: 12 November 2022

Publisher's Note: MDPI stays neutral with regard to jurisdictional claims in published maps and institutional affiliations.



Copyright: © 2022 by the authors. Licensee MDPI, Basel, Switzerland. This article is an open access article distributed under the terms and conditions of the Creative Commons Attribution (CC BY) license (<https://creativecommons.org/licenses/by/4.0/>).

1. Introduction

In recent years, haze weather has occurred frequently in China, and high-intensity air pollution has disturbed most cities, which has brought a serious threat to the sustainable economic and social development and the health of the people [1]. A high concentration of PM_{2.5} is an important factor affecting the formation of haze. PM_{2.5} in the air comes from socioeconomic factors such as urbanization dust, coal combustion, and automobile exhaust emissions. The concentration of PM_{2.5} is also closely related to natural and meteorological conditions such as topography, vegetation coverage, air pressure, humidity, and precipitation [2,3]. Therefore, it is important to promote the comprehensive management of the regional atmospheric environment, to ensure sustainable socioeconomic development, and to safeguard the health of people by exploring the evolution law and drive mechanism of PM_{2.5}.

Since 2008, there have been more and more researchers showing their concern with the theme of PM_{2.5}. On the spatial scale, they are mainly focused on single cities [4,5], urban agglomeration [6–8], basins [9–11], and countries [12,13]. For example, Zhou et al. [14] analysed the characteristics and driving factors of the spatio-temporal evolution of PM_{2.5} concentration in China from 2000 to 2011. Luna et al. [15] performed a spatial and temporal assessment of PM_{2.5} in the ambient air of Colombia. In the research content, the analyses are mainly regarding the physical and chemical properties, spatio-temporal evolution

trend, spatial heterogeneity, spatial agglomeration, influencing factors, and governance measures of PM_{2.5} [16–22]. For example, Li et al. [23] analysed the spatiotemporal evolution trend of PM_{2.5} concentration on the global scale. Jin et al. [24] analysed the relationship between the satellite-retrieved aerosol optical depth (AOD) and the PM_{2.5} concentration, as well as their spatio-temporal heterogeneity in the eastern United States from 2003 to 2017. Carmona et al. [25] analysed the influence of meteorological factors on PM_{2.5} concentration in northeastern Mexico. Casallas et al. [26] assessed the impact of policy implementation on PM_{2.5} in northwestern South America at different scales. In terms of research methods, the Moran index [27], geographical detector [28], spatial econometric model [29], land use regression (LUR) [30], geographically weighted regression (GWR) [31], data envelopment analysis (DEA) [32], generalized additive model (GAM) [33], STIRPAT [34] and LOESS [35], etc., were mainly used. For example, Xia et al. [36] used geographically weighted regression and a geographical detector to analyse the changing trend and determinants of PM_{2.5} concentration in the Yangtze River Economic Belt from 2000 to 2017. Londoño-Ciro and Cañón-Barriga [37] used geographically weighted regression and spatial econometric models to characterize the temporal and spatial distribution of the urban area of the city of Medellín-Colombia's PM_{2.5} concentration from 2013 to 2014. Kim et al. [38] evaluated the effect of the Particulate Matter Comprehensive Plan introduced by the Korean government to improve air quality, and proposed improvement measures. Generally speaking, the current studies mainly pay attention to the temporal and spatial distribution, evolution trend, influencing factors, and comprehensive governance of PM_{2.5} on the city, specific topography, or national scales, but there is little literature studying the effectiveness of comprehensive reform experimental areas in atmospheric environmental governance with PM_{2.5}.

Changsha–Zhuzhou–Xiangtan urban agglomeration is taken as the study area by this paper, which is one of the first comprehensive reform pilot areas for the construction of a resource-saving and environment-friendly society (also called a Two Oriented Society) in China. On the basis of the raster data of PM_{2.5} concentration from 2008 to 2019, retrieved from NASA atmospheric remote sensing images, we were concerned with problems of the construction of Two Oriented Society in this urban agglomeration from the grid scale, such as the temporal and spatial evolution characteristics, future development trends and driving factors of PM_{2.5} concentration. We used the gravity model, Moran index, Hurst index, and geographical detector in this study. It provides decision-making reference for the prevention and control of air pollution and the sustainable development of the economy and society.

2. Materials and Methods

2.1. Description of Changsha–Zhuzhou–Xiangtan Urban Agglomeration

Changsha–Zhuzhou–Xiangtan urban agglomeration is situated in the central and eastern parts of Hunan Province, including Changsha, Zhuzhou, and Xiangtan. The total area is about 2.8×10^4 km², which is a part of the region in the middle reaches of the Yangtze River (Figure 1). In 2018, the GDP of this region accounted for 41.98% of Hunan's GDP. It is the core growth pole of Hunan's economic development. With the rapid development of the economy, this region is also the most intense area of resource consumption and ecological destruction in Hunan Province. It is the key area for air pollution prevention and control in China. Changsha–Zhuzhou–Xiangtan urban agglomeration has a high topography to the east, south, and west, and a low topography to the north. It is a typical humid subtropical monsoon climate with distinct rains and heat in the same period, four seasons, rich precipitation, and uneven seasonal distribution. It is controlled by tropical depression in the summer, and has abundant precipitation. The wind direction is mostly southeast, which is conducive to the diffusion of PM_{2.5}. Winter is controlled by Mongolian high pressure, with less precipitation and mostly northwest wind, which easily leads to PM_{2.5} accumulation. In addition, it is an important heavy industrial base in China, involving many high-energy and high-pollution industries, such as iron and steel, non-ferrous metals,

construction machinery, automotive and parts, petrochemical, rail transit, and equipment manufacturing. Moreover, the main urban areas of Changsha, Zhuzhou, and Xiangtan are not more than 40 km apart, which also leads to the accumulation of $PM_{2.5}$ in the region. The government's analysis of $PM_{2.5}$ sources shows that the contribution rate of motor vehicle exhaust to $PM_{2.5}$ concentration is close to 25%, and that of industrial emissions is about 20%. The contribution rates of coal fume, dining fume, and fume are 11.6–12.9%, 10.2–14.3%, and 13.3–16.3%, respectively [39]. In 2009, the average annual $PM_{2.5}$ concentration was $62.26 \mu g/m^3$, which was much higher than the $10 \mu g/m^3$ standard set in the air quality guidelines issued by the World Health Organization (WHO) in 2005. The construction of the pilot area for the comprehensive reform of a Two Oriented Society provides not only a major opportunity but also an arduous challenge for the environmental protection work.

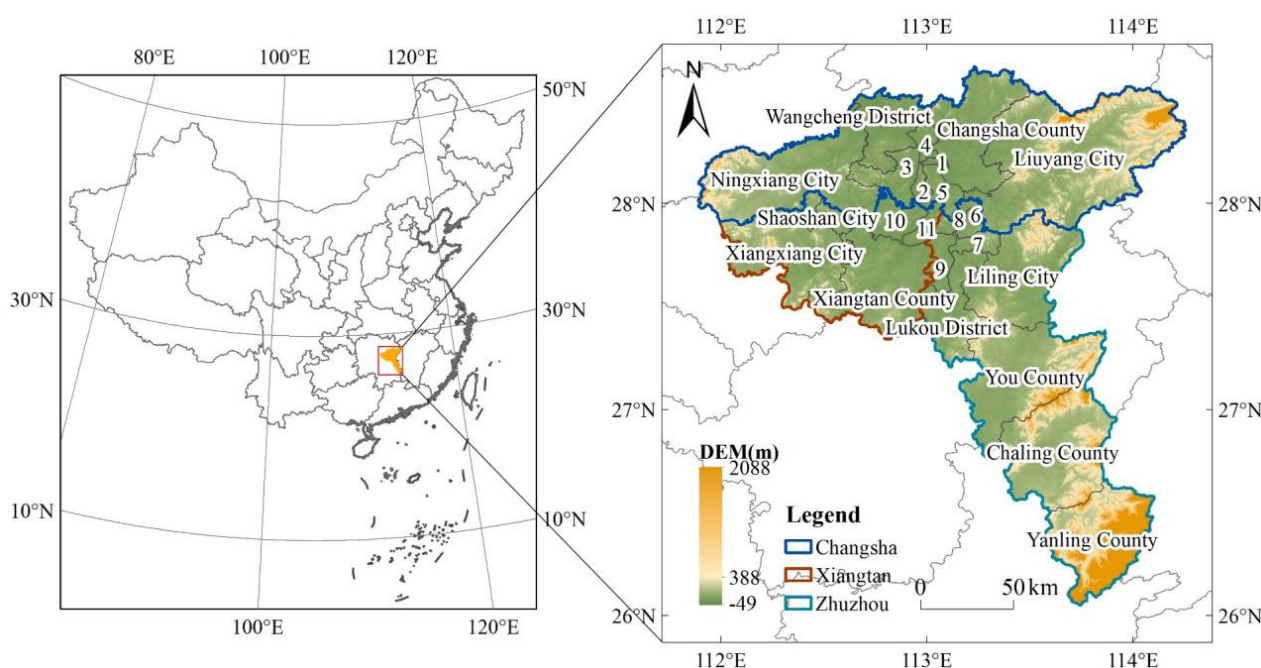


Figure 1. Geographic location of Changsha–Zhuzhou–Xiangtan urban agglomeration (1–11 stands for Furong District, Tianxin District, Yuelu District, Kaifu District, Yuhua District, Hetang District, Lousong District, Shifeng District, Tianyuan District, Yuhu District, and Yuetang district, respectively.).

2.2. Data

The data used in this study includes $PM_{2.5}$ concentration raster data, Changsha–Zhuzhou–Xiangtan urban agglomeration administrative boundary vector data, and driving factor data. (1) The annual $PM_{2.5}$ concentration raster data are retrieved from NASA Socioeconomic Data and Applications Centre (<https://sedac.ciesin.columbia.edu/>, accessed on 2 March 2022), from 2008 to 2019. Hammer et al. [40] verified their high accuracy (a resolution of $0.01^\circ \times 0.01^\circ$, $R^2 = 0.81$). Then, the raster data were smoothed for three years to ensure their stationarity and reliability. Hourly and monthly $PM_{2.5}$ concentration data were collected by reconstructing 6-hourly $PM_{2.5}$ datasets from 1960 to 2020 in China from Zenodo (<https://zenodo.org/>, accessed on 2 March 2022). (2) The administrative boundary vector data were taken from the Resource and Environmental Science and Data Centre of the Chinese Academy of Sciences (<https://www.resdc.cn/>, accessed on 2 March 2022). On the basis of the administrative boundary vector data, this study uses the fishing net tool of ArcGIS software to create a $3 \text{ km} \times 3 \text{ km}$ grid (a total of 3392 grids), calculates the average $PM_{2.5}$ concentration of each grid in each year, and establishes the spatial and temporal database of $PM_{2.5}$ concentration. (3) Driving factor data: eco-environmental quality data from China's historical 1 km resolution eco-environmental quality data (EEQ) from Zenodo;

night-time light index data from an extended time-series (2000–2018) of global NPP-VIIRS-like night-time light data from the Harvard Dataverse platform [41]; population density raster data from Scientific Data World Pop dataset (<https://hub.worldpop.org/>, accessed on 2 March 2022); altitude; leaf area index (LAI); normalized difference vegetation index (NDVI); and net primary productivity (NPP) data from the Resource and Environmental Science and Data Centre of the Chinese Academy of Sciences. The meteorological data of wind speed, pressure, precipitation rate, specific humidity, and temperature from China's meteorological forcing dataset (1979–2018) of the National Tibetan Plateau Data Centre were also used [42].

2.3. Methods

2.3.1. Gravity Model

The centre of gravity in geography refers to a point in regional space. The forces acting on the point in all directions remain relatively balanced. The movement of the centre of gravity can be used to reflect the changes in the spatial distribution of geographical objects and phenomena. Zhou et al. [14] studied spatial cluster characteristics of PM_{2.5} in China using a gravity model. In our study, the centre of gravity is calculated in order to reveal the PM_{2.5} pollution spatial migration process. Weight PM_{2.5} concentration centre of gravity in the study area is calculated by Equation (1):

$$\bar{X} = \frac{\sum_{i=1}^n (W_i \times S_i \times X_i)}{\sum_{i=1}^n (W_i \times S_i)}, \quad \bar{Y} = \frac{\sum_{i=1}^n (W_i \times S_i \times Y_i)}{\sum_{i=1}^n (W_i \times S_i)} \quad (1)$$

In this equation, \bar{X} is the longitude of the PM_{2.5} pollution centre of gravity. \bar{Y} is the latitude of the PM_{2.5} pollution centre of gravity. n is the total number of grids in the study area, and i is the grid serial number. X_i and Y_i are the longitude and latitude of the geometric centre of grid i , respectively. W_i represents the PM_{2.5} concentration of grid i , and S_i represents the area of grid i .

2.3.2. Spatial Autocorrelation

We used the global Moran's I index to test the average similarity of the spatial correlation of PM_{2.5} concentration in adjacent areas based on the size of the index. The calculation is performed using Equations (2) and (3):

$$S_0 = \sum_{i=1}^n \sum_{j=1}^n w_{ij} \quad (2)$$

$$I = \frac{n}{S_0} \times \frac{\sum_{i=1}^n \sum_{j=1}^n w_{ij} (C_i - \bar{C})(C_j - \bar{C})}{\sum_{i=1}^n (C_i - \bar{C})^2} \quad (3)$$

where I is the global Moran index and $I \in [-1, 1]$. When $I \in (0, 1]$, it shows that the research unit has a positive spatial autocorrelation; the higher the value is, the stronger the spatial aggregation of PM_{2.5} concentration is. When $I \in [-1, 0)$, it shows that the research unit has a negative spatial autocorrelation; the smaller the value is, the stronger the spatial discreteness of PM_{2.5} concentration is. When $I = 0$, there is no correlation between study units. n is the number of study units. C_i and C_j denote the PM_{2.5} concentration values of the i and j study units, respectively. \bar{C} is the average PM_{2.5} concentration of all study units. w_{ij} is the spatial weight value (when unit i is next to j , $w_{ij} = 1$; when not adjacent, $w_{ij} = 0$).

Local Moran's I is used to reveal the local spatial autocorrelation of PM_{2.5} concentration, that is, the degree of correlation between the PM_{2.5} concentration of a study unit and the adjacent unit. The calculation equation is shown in Equation (4).

$$I_i = \frac{n(C_i - \bar{C})}{\sum_{i=1}^n (C_i - \bar{C})^2} \sum_{j=1}^m w_{ij} (C_j - \bar{C}), (i \neq j) \quad (4)$$

where I_i is the local Moran index; n is the total number of spatial units; m is the number of cities geographically adjacent to the spatial unit i ; C_i and C_j represent the $PM_{2.5}$ concentration of the spatial unit i and spatial unit j , respectively; \bar{C} is the average $PM_{2.5}$ concentration of all spatial units; and w_{ij} is the spatial weight value. At the same time, the standardized counter Z is often used to test the significance of the Moran index. The standardized counter of the Moran index is defined as Equation (5):

$$Z(I) = \frac{[I - E(I)]}{\sqrt{Var(I)}} \quad (5)$$

where $Z(I)$ is the significance level of global Moran's I , $Var(I)$ is the variance of global Moran's I , and $E(I)$ is the mathematical expectation of global Moran's I . Taking 99% confidence as an example, when $Z(I) < -2.58$, it shows that $PM_{2.5}$ concentration has the characteristics of negative correlation in spatial distribution, including "low-high" correlation and "high-low" correlation; when $-2.58 \leq Z(I) \leq 2.58$, it shows that $PM_{2.5}$ concentration has no spatial autocorrelation and an independent random distribution. When $Z(I) > 2.58$, it shows that $PM_{2.5}$ concentration presents the characteristics of positive correlation in spatial distribution, including "high-high" aggregation and "low-low" aggregation, which is also called hot spot and cold spot distribution.

2.3.3. Hurst Index

In this study, the Hurst index (H) is used to predict the future evolution trend of $PM_{2.5}$ concentration in various portions of the study area. The Hurst index is proposed by the British scholar Hurst to quantitatively describe the long-range similarity or persistence of the time series. Generally, it is calculated by the method of R/S. The time series for obtaining the response at times t_1, t_1, \dots, t_n are T_1, T_1, \dots, T_n . For any positive integer $\tau \geq 1$, the average of the time series is calculated by Equation (6):

$$\langle T \rangle_\tau = \frac{1}{\tau} \sum_{t=1}^{\tau} T(t), \tau = 1, 2, 3, \dots, n \quad (6)$$

The cumulative deviation expressed by $X(t)$ is calculated by Equation (7):

$$X(t, \tau) = \sum_{\mu=1}^t (T(\mu) - \langle T \rangle_\tau) \quad 1 \leq t \leq \tau \quad (7)$$

The difference between the maximum $X(t)$ value and the minimum $X(t)$ value corresponding to the same τ value is turned into a range, which is recorded as Equation (8):

$$R(\tau) = \max_{1 \leq t \leq \tau} X(t, \tau) - \min_{1 \leq t \leq \tau} X(t, \tau), \tau = 1, 2, 3, \dots, n \quad (8)$$

The standard deviation $S(\tau)$ is calculated by Equation (9):

$$S(\tau) = \left[\frac{1}{\tau} \sum_{t=1}^{\tau} (T(t) - \langle T \rangle_\tau)^2 \right]^{1/2} \quad \tau = 1, 2, 3, \dots, n \quad (9)$$

The final R/S is calculated by Equation (10):

$$R/S = (\tau/2)^H \quad (10)$$

where H is the Hurst index. When $0.5 < H < 1$, it means that the long-term correlation feature of the sequence is positive persistence, and the future change trend is the same as the current change trend. The closer to 1 the H value is, the stronger the positive persistence is. When $0 < H < 0.5$, it means that the long-term correlation of the time series is characterized by anti-persistence. The future change trend is opposite to the current change trend. The

closer to 0 the H value is, the stronger the anti-persistence is. When $H = 0.5$, it means that the future change trend of the time series is random and independent of the present.

2.3.4. Geographical Detector

Spatial differentiation is one of the basic characteristics of geographical phenomena and the spatial expression of natural and socio-economic processes. As a powerful tool to detect spatial differentiation and reveal the driving factors of spatial differentiation, the geographical detector has the characteristics of a nonlinear hypothesis, elegant form, and clear physical meaning. At present, it has been widely used in the fields of ecology, meteorology, hydrology, social economy, and so on [43]. The geographical detector covers four aspects: interactive detection, ecological detection, factor detection, and risk detection. The principle is to analyse the spatial stratification heterogeneity of each factor by comparing the interlayer variance and total variance of each factor, in order to explore the driving force of each factor on the dependent variable. This paper mainly uses factor detection and interactive detection to calculate the explanation degree of factors to the spatial differentiation of $PM_{2.5}$ concentration in the study area. It also reveals its spatial differentiation mechanism.

Factor detection uses q statistics to characterize the explanatory power of each factor for the dependent variable. The value of q means that the independent variable X explains $100 \times q\%$ of the spatial differentiation of $PM_{2.5}$ concentration. The expression is shown in Equations (11) and (12):

$$q = 1 - \frac{\sum_{h=1}^L N_h \sigma_h^2}{N \sigma^2} = 1 - \frac{SSW}{SST} \quad (11)$$

$$SSW = \sum_{h=1}^L N_h \sigma_h^2, SST = N \sigma^2 \quad (12)$$

where h is the stratification of independent variable X or $PM_{2.5}$ concentration Y ; N_h and N are the number of units in layer h and the whole area, respectively; and σ_h^2 and σ^2 are the variance of the layer h and Y values of the whole region. SSW and SST are the sum of intra-layer variance and total variance of the whole region, respectively. The value range of q is between 0–1. The larger its value is, the higher the explanatory degree of the independent variable to the dependent variable is.

Interaction detection is used to identify the interaction between different factors, that is, to evaluate whether the joint action of the two factors will enhance or weaken the explanatory power of dependent variables. When $q(x_1 \cap x_2) < \min(q(x_1), q(x_2))$, it indicates that the type of the two-factor interaction is nonlinear weakening. When $\min(q(x_1), q(x_2)) < q(x_1 \cap x_2) < \max(q(x_1), q(x_2))$, it indicates that the type of the two-factor interaction is unidirectional weakening. When $q(x_1 \cap x_2) > \max(q(x_1), q(x_2))$, it indicates that the type of the two-factor interaction is a bidirectional enhancement. When $q(x_1 \cap x_2) > q(x_1) + q(x_2)$, it indicates that the type of the two-factor interaction is a nonlinear enhancement. When $q(x_1 \cap x_2) = q(x_1) + q(x_2)$, it indicates that the two factors are independent of each other.

3. Results

3.1. Spatio-Temporal Evolution Characteristics of $PM_{2.5}$ Concentration

3.1.1. Characteristics of Time Evolution

The concentration of $PM_{2.5}$ showed an inverted U-shaped trend from 2009 to 2018 (Figure 2). Before 2011, the average annual $PM_{2.5}$ concentration showed an upward trend, from $62.26 \mu g/m^3$ in 2009 to $63.6 \mu g/m^3$ in 2011, with an average annual growth rate of 1.08%. In 2011, the State Council successively issued the Circular on the Planning of National Main Functional Areas and the Circular on the 12th Five-year Plan of National Environmental Protection. Since then, documents on the prevention and control of air pollution in key areas have been issued, such as the 12th Five-year Plan and the Environmental Air Quality Standard, and the average annual $PM_{2.5}$ concentration has shown a steady downward trend. It dropped from $63.6 \mu g/m^3$ in 2011 to $41.4 \mu g/m^3$ in 2018, with

an average annual decrease of 4.99%, indicating that the decline in PM_{2.5} concentration is closely related to the national environmental functional zoning for air pollution prevention and control, environmental quality monitoring and assessment system, pollution reduction statistics, monitoring and assessment system, and comprehensive control of a variety of air pollutants. In particular, after the State Council approved the implementation of the Action Plan for the Prevention and Control of Air Pollution in 2014 and the notice of the 13th Five-Year Plan issued in 2016, the concentration of PM_{2.5} decreased significantly by 7.98% and 10.95%, respectively, in 2013 and 2016. According to the air quality guidelines issued by the World Health Organization (WHO) in 2009 and the PM_{2.5} concentration standard classified by China's Environmental Air Quality Standard (GB3095-2012), and combined with the actual situation of this urban agglomeration, the PM_{2.5} concentration grade of this area is divided into six grades. The area ratio of each PM_{2.5} concentration grade from 2009 to 2018 (Figure 2) is calculated. Meanwhile, a linear fitting model ($y = -2.6734x + 69.305$) is constructed in years.

The results show the following. (1) The proportion of areas with PM_{2.5} concentration which is lower than $35 \mu\text{g}/\text{m}^3$ (the average annual limit of China Environmental Air Quality Standard) increased from 0% in 2009 to 10.38% in 2018. The proportion of areas where it is higher than $75 \mu\text{g}/\text{m}^3$ increased from 0% in 2009 to 2.36% in 2011, and then decreased rapidly to 0% in 2013. (2) The proportion of areas with a PM_{2.5} concentration which is lower than $50 \mu\text{g}/\text{m}^3$ increased from 11% in 2013 to 99.73% in 2018, showing an increase of more than eight times, which was the most obvious increase in 2017–2018. (3) The proportion of areas with PM_{2.5} concentrations between $50\text{--}75 \mu\text{g}/\text{m}^3$ decreased from 88.74% in 2009 to 0.27% in 2018, with the most obvious decrease in 2013–2017. (4) Compared with 2009, the PM_{2.5} concentration in all areas decreased by various degrees in 2018. The biggest areas, where the PM_{2.5} concentration decreased by two grades, accounts for 90.63%. The following areas where the PM_{2.5} concentration decreased by three grades account for 7.84%, and the last areas, where the PM_{2.5} concentration decreased by one grade, account for 1.53%. (5) According to the linear fitting model ($\mu\text{g}/\text{m}^3$), the PM_{2.5} concentration shows a significant decline (negative) trend ranging from -3.32 to $-2.03 \mu\text{g}/\text{m}^3$ per year. (6) The PM_{2.5} concentration is low in the daytime and higher at night. The highest concentration occurs at 8:00 in the morning. Because there is an obvious temperature inversion in the lower atmosphere at night, it is easy for PM_{2.5} to accumulate [44]. In addition, the morning is the peak time for people to travel, and there is a significant amount of vehicle exhaust emissions, leading to the highest PM_{2.5} concentration. (7) The PM_{2.5} concentration is highest in the winter and lowest in the summer. We believe that this is related to terrain conditions and wind patterns. The study area is typically located in the inland, with a horseshoe-shaped structure with the opening facing north. The dominant wind direction of the city throughout the year is northwest. The urban wind speed is relatively small in autumn and winter, which is not conducive to the diffusion of air pollutants. However, affected by the southeast monsoon in the summer, it is conducive to PM_{2.5} diffusion [45].

3.1.2. Spatial Evolution Characteristics of the PM_{2.5}

On the basis of the PM_{2.5} concentration data of Changsha–Zhuzhou–Xiangtan urban agglomeration from 2009 to 2018, $3 \text{ km} \times 3 \text{ km}$ fishing nets (a total of 3392 grids) were created by using ArcGIS software, the average annual PM_{2.5} concentration of each grid was calculated, and the spatial distribution maps of PM_{2.5} concentration in 2009, 2011, and 2018 of this study area (Figure 3) were drawn. From 2009 to 2018, the spatial distribution of PM_{2.5} concentration was quite different, showing a spatial distribution pattern which was high in the west and low in the east, high in the north and low in the south, and decreasing from northwest to southeast. Regional differences showed the characteristics of expanding at first, and then shrinking. Taking $50 \mu\text{g}/\text{m}^3$ (the third grade PM_{2.5} concentration limit) as the dividing point, the PM_{2.5} concentration is divided into a high-value area and a low-value area.

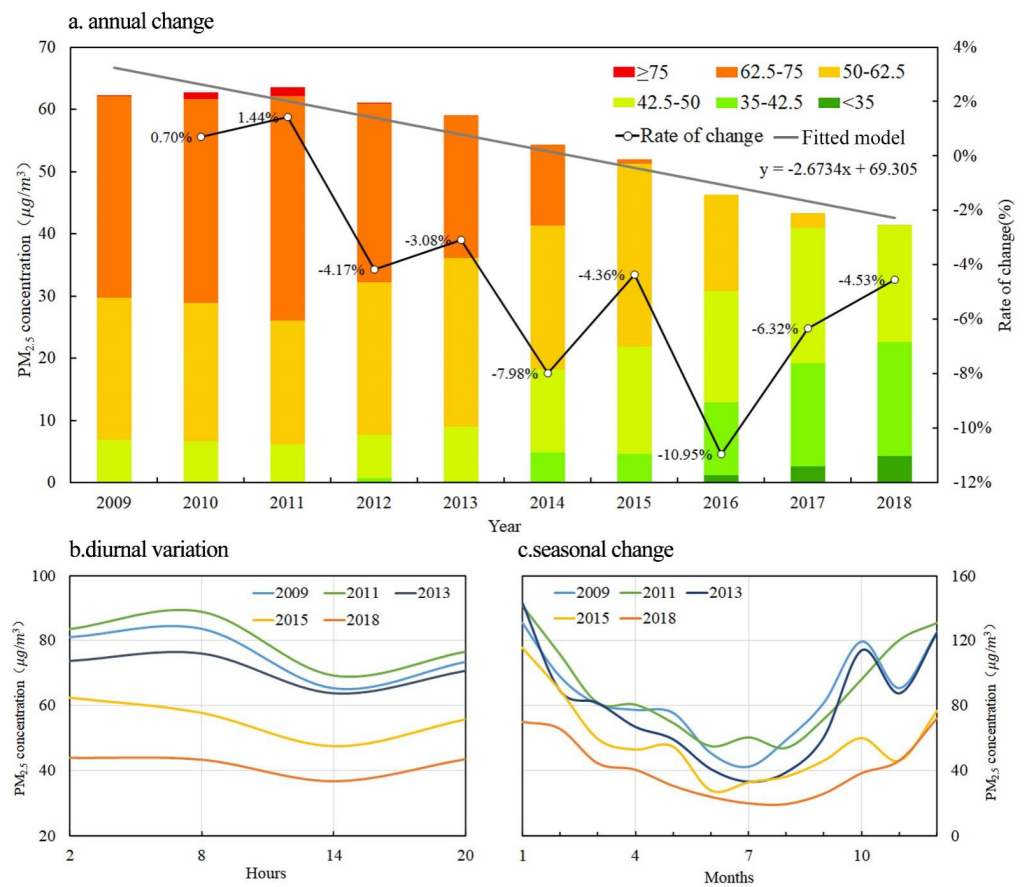


Figure 2. Spatial Evolution of PM_{2.5} concentration in Changsha–Zhuzhou–Xiangtan urban agglomeration from 2009 to 2018. (a) Annual change; (b) diurnal variation; (c) seasonal change. Remarks: (a) The left coordinate describes the annual change of PM_{2.5} concentration, which is represented by a histogram (the height of different colours represents the annual area proportion of different PM_{2.5} concentration grades). The right coordinate describes the annual growth rate, which is represented by black lines.

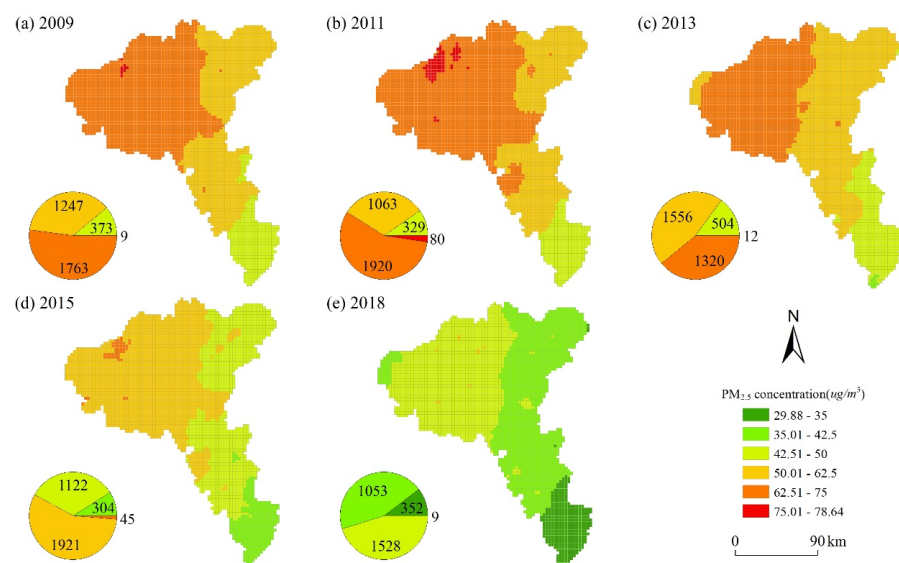


Figure 3. Spatial variation of annual average PM_{2.5} concentration. (a) 2009, (b) 2011, (c) 2013, (d) 2015, (e) 2018. The pie chart at the lower left corner shows the annual area proportion of concentrations.

The spatial distribution difference of PM_{2.5} concentration is mainly reflected as follows. (1) The PM_{2.5} concentration has obvious agglomeration and distribution characteristics. The high-value areas are primarily scattered in the low-lying and economically developed areas such as Xiangtan City, Changsha City, and Zhuzhou City in the northwest, and the low-value areas are primarily scattered in the high-lying areas of Liuyang, You County, Chaling County, and Yanling County in the east and south, indicating that PM_{2.5} concentration is closely related to topography and economic development. (2) In 2009, 89% of this urban agglomeration was in the area with a high PM_{2.5} concentration, and 0.27% of the areas had a PM_{2.5} concentration over 75 µg/m³, which is distributed in the main urban area of Ningxiang City. The whole territory of Yanling County is a low-value area, and some low-value areas are also distributed in some high-lying areas of Chaling County and You County. (3) The high-value area of PM_{2.5} concentration showed a trend of diffusion from 2009 to 2011. In 2011, 90.3% of the areas were high-value areas, and 2.36% were higher than 75 µg/m³, primarily distributed in the main urban areas and agricultural areas of Ningxiang City and Wangcheng District. (4) In 2018, 99.73% of areas had low PM_{2.5} concentration, indicating that the air pollution control actions taken by the government achieved practical results in key areas after the introduction of a series of policies including the 12th Five-Year Plan for the Prevention and Control of Air Pollution. With the development of the social economy, the concentration of PM_{2.5} increased at first, and then decreased. It is worth noting that 0.27% of the areas still had a PM_{2.5} concentration over 50 µg/m³, scattered in the heavily populated areas of districts and counties in the northwest of this urban agglomeration in 2018.

3.2. Spatio-Temporal Migration Characteristics of PM_{2.5} Concentration

In geography, the geographical centre of gravity is the vector resultant point that describes the geographical attributes or the distribution of things [46]. In this study, on the basis of the annual PM_{2.5} concentration grid data of Changsha—Zhuzhou—Xiangtan urban agglomeration, the longitude and latitude coordinates of the annual PM_{2.5} concentration centre of gravity are calculated by Equation (1), and the result is shown in Figure 4. The results show that the centre of gravity of PM_{2.5} concentration from 2009 to 2018 was situated in Lukou District of Zhuzhou City, and the interannual change is obvious. From 2009 to 2011, the centre of gravity moved about 0.58 km to the east-north of 24.8°, with an average annual moving distance of about 0.57 km. According to “Hunan Province 13th Five-Year Plan for Environmental Protection,” compiled by the Ecology and Environment Department of Hunan (EEDH), the economy of Changsha—Zhuzhou—Xiangtan urban agglomeration was in a stage of rapid development, with an average annual gross domestic product growth rate of 22.09%. There were too many enterprises with high pollution and energy consumption during this stage. They further increased the concentration of PM_{2.5} in this region [47]. From 2011 to 2014, the centre of gravity moved about 1.25 km to the southwest, with an average annual shift of 0.61 km. During this period, Changsha—Zhuzhou—Xiangtan urban agglomeration issued and implemented “Environmental Co-governance Planning for Changsha—Zhuzhou—Xiangtan urban agglomeration (2010–2020).” It advocated for the vigorous development of clean energy sources such as natural gas, wind energy, and solar energy, and, meanwhile, reduced the proportion of coal used in primary energy, and carried out comprehensive control actions for pollutants such as sulphur dioxide as well as smoke and dust produced by the iron and steel, non-ferrous, chemical, building materials, and other industries [48]. From 2014 to 2018, the centre of gravity moved 2.36 km to the southeast by 34.37°, with an average annual shift of 0.78 km. During the implementation of “the 13th Five-Year Plan for Eco-environmental Protection,” Hunan Province successively issued a series of policies and regulations, such as the “Regulations on Responsibility for Eco-environmental Protection in Hunan Province” and the “Measures for Responsibility for Major Eco-environmental Problems (Events) in Hunan Province,” which improved the system for the prevention and control of atmospheric pollution. They closed more than 1000 highly polluting enterprises and further optimized the industrial

structure. Emissions of sulphur dioxide and nitrogen oxides decreased by 28.7% and 18.8%, respectively, compared with 2015. Significant achievements have been made in the prevention and control of air pollution [49].

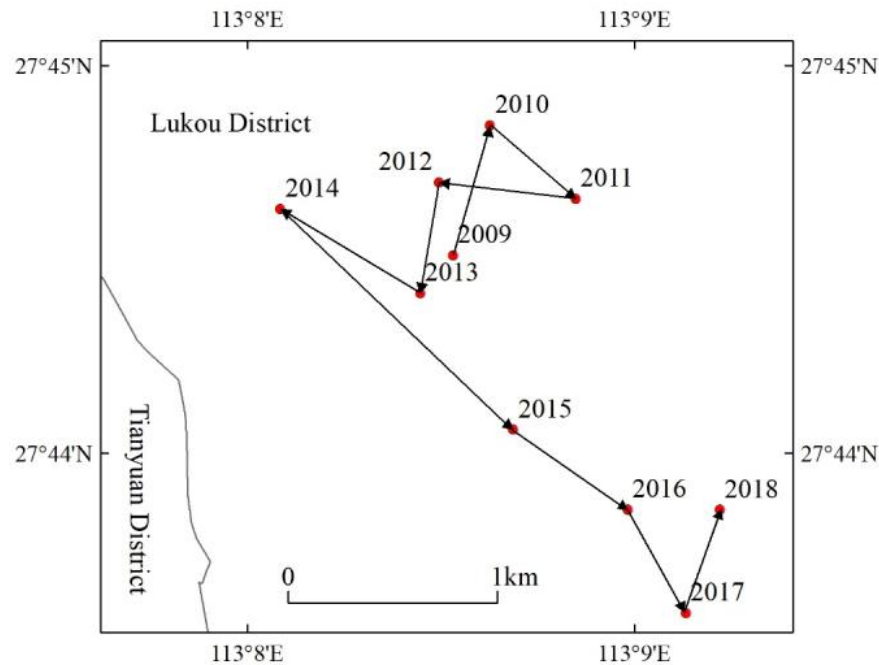


Figure 4. Change trend of PM_{2.5} concentration centre of gravity in Changsha—Zhuzhou—Xiangtan urban agglomeration from 2009 to 2018.

3.3. Spatial Agglomeration Characteristics of PM_{2.5} Concentration

3.3.1. Global Spatial Autocorrelation Feature

According to the global Moran's I calculation equations and using ArcGIS's Spatial statistics tools, it was calculated that the statistical values of Moran's I of PM_{2.5} concentration of Changsha—Zhuzhou—Xiangtan urban agglomeration in 2009, 2011, 2013, 2015, and 2018 were 0.986 ($Z = 79.80$), 0.984 ($Z = 79.66$), 0.988 ($Z = 79.97$), 0.984 ($Z = 79.69$), and 0.983 ($Z = 79.58$), respectively. The results show that the statistical values of Moran's I are all positive and greater than 0.98, and that it has passed the significance test threshold level of 1%. They also show that the PM_{2.5} concentration has a strong spatial correlation, and that areas with high PM_{2.5} concentrations are often distributed together.

3.3.2. Local Spatial Autocorrelation Analysis

Using ArcGIS clustering and outlier analysis tools, we calculated the local Moran's I (Figure 5) of 3392 grids of the study area in 2009, 2011, 2013, 2015, and 2018. The grid cells showing significant local spatial autocorrelation were divided into four types: High–High Cluster, High–Low Outlier, Low–High Outlier, and Low–Low Cluster. The results show that the concentration of PM_{2.5} in more and more areas of the region from 2009 to 2018 showed strong spatial aggregation. The types of spatial aggregation are “High–High Cluster” and “Low–Low Cluster,” showing a strong positive autocorrelation. The proportion of hot spots increased from 28.57% in 2009 to 29.39% in 2018, with an average annual increase of 0.29%. The proportion of cold spot areas increased from 19.13% in 2009 to 23.29% in 2018, with an average annual increase of 2.17%. The proportion of cold spot areas and hot spot areas showed an upward trend, and the rising speed of cold spot areas was faster. From a spatial point of view, the hot spot areas were concentrated in the areas with heavy industrial pollution and vehicle exhaust emissions, such as the whole of Xiangtan City and the west of Changsha City. The cold spot areas were concentrated in the high-lying and underdeveloped areas, such as the south of Zhuzhou City and the east of

Liuyang City. The southwest of Chaling County was a cold spot distribution area in 2009 and 2011, but it had no characteristic point distribution in 2018. Agricultural non-point source pollution and straw burning may be the reasons for the deterioration of air quality in this area [50]. The southeast of Liuyang City had no characteristic point distribution in 2009 and 2011, but in 2018, it was a cold spot distribution area. The air quality has been significantly improved, indicating that the prevention and control of air pollution in this area has achieved remarkable results [51].

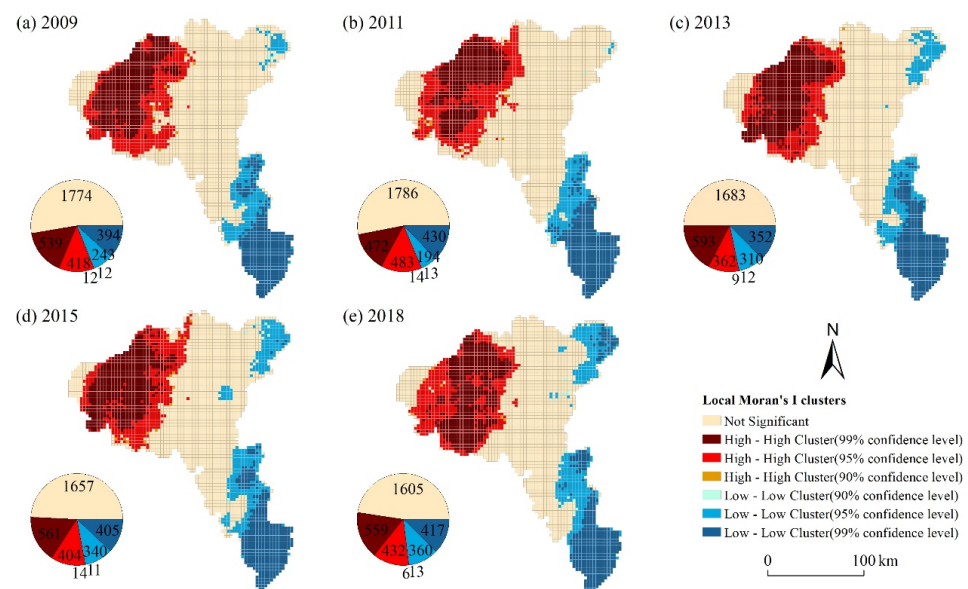


Figure 5. Local autocorrelation of $PM_{2.5}$ concentration in (a) 2009, (b) 2011, (c) 2013, (d) 2015, and (e) 2018. The pie chart at the lower left corner shows the annual area proportion of clusters.

3.4. Future Development Trend of $PM_{2.5}$ Concentration

On the basis of the $PM_{2.5}$ concentration data of the study area from 2009 to 2018, each grid Hurst index is calculated with the aid of Equation (6–10). Combined with the characteristics of the Hurst index and natural breakpoint method, the results are classified in Figure 6. It can be noted that the Hurst index of each area of this region ranges from 0.46 to 0.97. The regional difference is obvious. The high-value areas are mainly distributed in Xiangtan City and Changsha City. The low value areas are mainly distributed in Zhuzhou City, as well as in the central and eastern parts of Changsha City. The areas with a Hurst index greater than 0.5 account for 99.76%, indicating that the $PM_{2.5}$ concentration in most areas is positively persistent. There is an obvious Hurst phenomenon, that is, the future $PM_{2.5}$ concentration in most areas of this region is very likely to continue the trend of a gradual decline in $PM_{2.5}$ concentration which has been observed in the past [52]. It should be noted that the Hurst index of 0.24% of the areas is less than 0.5. These are mainly distributed in some rural areas of Chaling County and Yanling County, indicating that the non-point source pollution caused by agricultural development will lead to the future evolution of $PM_{2.5}$ concentration in these areas. The future trend is contrary to the continuous decline in $PM_{2.5}$ concentration in the past.

3.5. Spatial Differentiation Mechanism of $PM_{2.5}$ Concentration

The spatial difference of $PM_{2.5}$ concentration in Changsha–Zhuzhou–Xiangtan urban agglomeration is significant. The reasons are difficult to discern, and the driving factors may be various. Past research has found that the driving factors are related to natural factors, such as topography, vegetation, and forest fires. They are also related to human factors, such as industrial soot emissions, coal burning, and motor vehicle exhaust. At the same time, they are also closely related to meteorological factors like rainfall, temperature, and air pressure. In this study, we formulated the rules for screening driving factors for

spatial differentiation of PM_{2.5} concentration in this urban agglomeration based on the relevant research results [53,54], and considering the actual situation of the study area and the availability of data. We selected the following 13 driving factors which contributed greatly to the spatial differentiation of PM_{2.5} concentration from three aspects: natural conditions, socio-economic conditions, and meteorology. These are altitude (X₁), slope (X₂), eco-environmental quality (EEQ) (X₃), normalized difference vegetation index (NDVI) (X₄), leaf area index (LAI) (X₅), net primary productivity (NPP) (X₆), population density (X₇), night-time light index (X₈), wind speed (X₉), pressure (X₁₀), precipitation rate (X₁₁), specific humidity (X₁₂), and temperature (X₁₃).

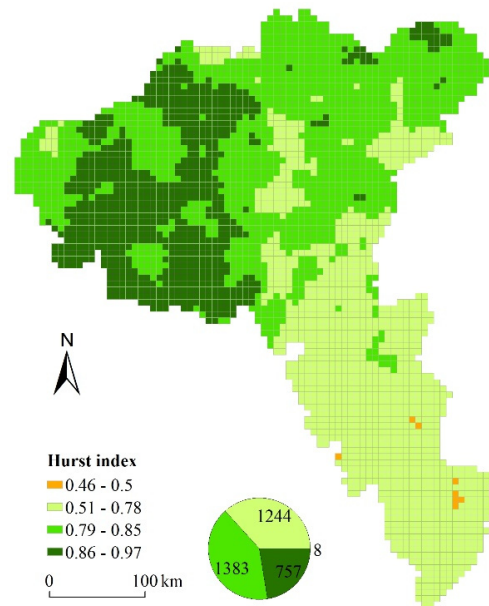


Figure 6. Hurst index of Changsha–Zhuzhou–Xiangtan Urban agglomeration in 2009–2018.

3.5.1. Factor Detection

In order to more accurately analyse the driving factors of spatial differentiation of PM_{2.5} concentration in Changsha–Zhuzhou–Xiangtan urban agglomeration, this study used ArcGIS software to create a 3 km × 3 km fishing net (with a total of 3392 grids), and calculated the observations of the 13 driving factors in each grid. Then, we used the Jenks natural breakpoint method to divide the observations of the driving factors in each grid into six categories. In the end, we imported the discrete data into the geographic detector for factor detection and interactive detection. The factor detection results can be seen in Table 1.

Table 1. Factor detection result analysis over 5 years.

Driving Factor	2009		2011		2013		2015		2018		Average Value	
	<i>q</i>	<i>p</i>	<i>q</i>	<i>p</i>	<i>q</i>	<i>p</i>	<i>q</i>	<i>p</i>	<i>q</i>	<i>p</i>		
Natural condition	Altitude (X ₁)	0.55	0.00	0.55	0.00	0.50	0.00	0.50	0.00	0.58	0.00	0.40
	Slope (X ₂)	0.42	0.00	0.41	0.00	0.39	0.00	0.40	0.00	0.45	0.00	
	Eco-environmental quality (X ₃)	0.49	0.00	0.44	0.00	0.45	0.00	0.47	0.00	0.53	0.00	
	NDVI (X ₄)	0.20	0.00	0.27	0.00	0.36	0.00	0.34	0.00	0.31	0.00	
	LAI (X ₅)	0.55	0.00	0.54	0.00	0.53	0.00	0.54	0.00	0.60	0.00	
Socioeconomic status	NPP (X ₆)	0.11	0.00	0.09	0.00	0.12	0.00	0.12	0.00	0.13	0.00	0.08
	Population density (X ₇)	0.09	0.01	0.09	0.00	0.08	0.03	0.08	0.20	0.10	0.15	
	Night-time light index (X ₈)	0.03	1.00	0.05	0.99	0.07	0.36	0.07	0.67	0.14	0.00	
	Wind speed (X ₉)	0.39	0.00	0.09	0.00	0.11	0.00	0.18	0.00	0.07	0.00	
Meteorology	Pressure (X ₁₀)	0.54	0.00	0.55	0.00	0.50	0.00	0.49	0.00	0.58	0.00	0.32
	Precipitation rate (X ₁₁)	0.14	0.00	0.57	0.00	0.53	0.00	0.52	0.00	0.42	0.00	
	Specific humidity (X ₁₂)	0.24	0.00	0.11	0.00	0.09	0.00	0.26	0.00	0.21	0.00	
	Temperature (X ₁₃)	0.28	0.00	0.32	0.00	0.30	0.00	0.29	0.00	0.30	0.00	

Note: *q* represents the driving force of each driving factor, and *p* represents the significant level of each driving factor.

The driving effect of night-time light index (X_8) in 2009, 2011, 2013, and 2015 and that of population density (X_7) in 2015 and 2018 were not significant, while the other driving factors had a significant impact on the spatial differentiation of $PM_{2.5}$. The driving forces for each factor are quite different. According to the five-year average Q value, the explanatory power of each driving factor to the spatial differentiation of $PM_{2.5}$ concentration was as follows: LAI (0.564) > altitude (0.559) > pressure (0.556) > eco-environmental quality (0.487) > slope (0.426) > precipitation rate (0.377) > temperature (0.299) > NDVI (0.260) > specific humidity (0.188) > wind speed (0.185) > NPP (0.108) > population density (0.093) > night-time light index (0.072).

The average Q value of the natural condition driving factor was 0.40, which shows an upward trend, indicating that it plays a dominant role in the spatial differentiation of $PM_{2.5}$ concentration. The average Q value of meteorological driving factors was 0.32. Its annual change is small, which indicates that it plays a key role in the spatial differentiation of $PM_{2.5}$ concentration. The average Q value of the driving factors for the socio-economic status was only 0.08, which is relatively low. However, in 2009–2018, the average Q value increased by 95.04%, which meant that it was a rapid driving force for the spatial difference of $PM_{2.5}$.

From the point of view of natural conditions, the western and northern parts of this urban agglomeration have low topography and gentle slope. $PM_{2.5}$ gathers easily here, and does not easily spread due to the surrounding mountains, which leads to the increase in $PM_{2.5}$ concentration in the area. Low vegetation coverage and vegetation quality are also important reasons for the high $PM_{2.5}$ concentration in this region. Vegetation can directly reduce the concentration of $PM_{2.5}$ in the air by adsorption and blocking, or it can indirectly reduce the concentration of $PM_{2.5}$ by leaf transpiration, increasing atmospheric humidity, and absorbing and transforming sulphur, lead, and other metals and nonmetals in the air. Increasing vegetation coverage and improving vegetation quality are important ways to reduce $PM_{2.5}$ concentration.

In terms of social and economic conditions, population density and night-time light index are the driving factors for regional population and economic vitality. Their driving force for the $PM_{2.5}$ spatial differentiation is weak, but they are on the rise. The reasons are as follows: The secondary industry accounted for a high proportion in Xiangxiang City, Xiangtan County, Ningxiang City, and other areas at the initial stage of the establishment of the Two Oriented Society. Industrial soot emissions are significant, and contribute greatly to the $PM_{2.5}$ concentration. In contrast, the population density in these areas is relatively low. Its influence on $PM_{2.5}$ concentration is also relatively small. With the gradual progress of the construction of the Two Oriented Society, the industrial structure of this urban agglomeration is gradually upgraded and rationalized. Polluting enterprises are optimized and eliminated, and industrial pollution decreases year by year. Its driving force on $PM_{2.5}$ concentration gradually decreases. Meanwhile, the driving force of population and economic vitality increases rapidly.

From a meteorological point of view, pressure has the strongest driving force on the spatial differentiation of $PM_{2.5}$ concentration ($Q > 0.5$). Air pressure is the atmospheric pressure acting on a unit area, which is closely associated with the situation of atmospheric circulation. The surrounding high-pressure air masses flow to the centre when the local surface is controlled by low pressure, resulting in an updraft in the centre. The increasing wind force is advantageous to the upward evacuation of pollutants, and the $PM_{2.5}$ concentration is lower. On the contrary, there is a downdraft in the centre if the ground is controlled by high pressure, which inhibits the upward diffusion of pollutants. Under the control of stable high pressure, pollutants accumulate and $PM_{2.5}$ concentration increases [55]. The average driving forces of precipitation rate and temperature are 0.377 and 0.299, respectively, which are also at a high level. Precipitation can effectively reduce the concentration of $PM_{2.5}$, but the process is slow. The driving forces of wind speed and specific humidity are relatively low. Previous studies have pointed out that wind direction affects the long-distance transport of $PM_{2.5}$ [56]; the government's analysis of the source of $PM_{2.5}$ concentration also indicates that about 10% of the fine particles in the Changsha–Zhuzhou–Xiangtan urban agglomeration come from the surrounding areas [39].

3.5.2. Interactive Detection

The interactive detection results of spatial differentiation of PM_{2.5} concentration in Changsha–Zhuzhou–Xiangtan urban agglomeration (Figure 7) show that the driving force of the interaction of any two driving factors on the spatial differentiation of PM_{2.5} concentration is greater than that of a single driving factor. The main types of pairwise interaction are two-factor enhancement and nonlinear enhancement, indicating that the spatial differentiation of PM_{2.5} concentration is not caused by a single influence factor; it is the result of the joint action of different factors [57]. Among them, the driving force of pressure ∩ specific humidity was the strongest, and the *q* value of this factor interaction was the highest at 0.75 in 2009. The *q* value of wind speed ∩ precipitation rate reached 0.89 in 2011 and 2015, which was the strongest driving force for the spatial differentiation of PM_{2.5} concentration. The driving force of LAI ∩ precipitation rate was the strongest in 2018, and the *q* value of this factor interaction was at its highest at 0.76. The driving forces of the following two-factor interactions on the spatial differentiation of PM_{2.5} concentration are greater than 0.8: altitude ∩ precipitation rate, LAI ∩ precipitation rate, and pressure ∩ precipitation rate in 2011 and 2013, and specific humidity ∩ precipitation rate in 2015. It also can be seen that the driving force of two factors is stronger than that of a single factor in the spatial differentiation of PM_{2.5} concentration, although other driving factors all have forces less than 0.8.

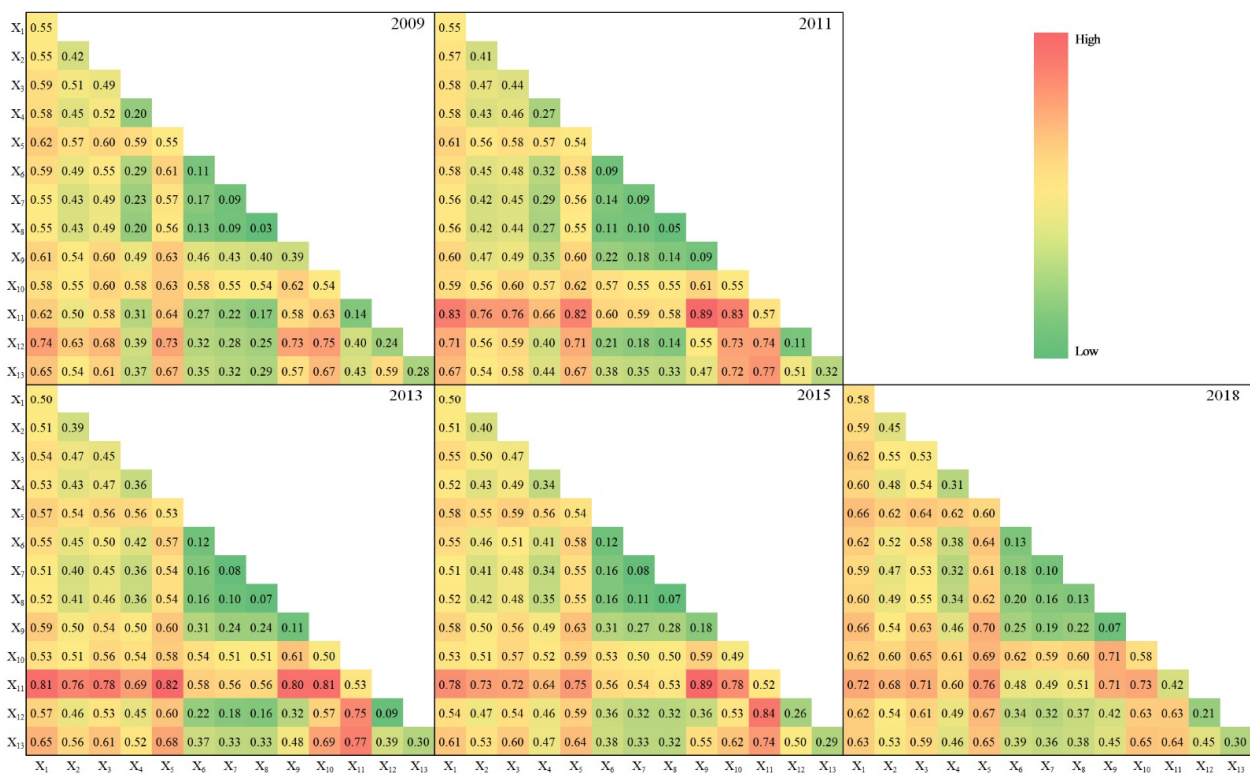


Figure 7. Interactive detection results between factors in 2009, 2011, 2013, 2015, and 2018.

4. Discussion

The Environmental Kuznets Curve (EKC) theory shows that environmental pollution presents an inverted U-shaped development trend with the development of social economy [58]. Our study confirms this point of view.

Past research has suggested that population density is positively associated with PM_{2.5} concentration [59]. In this study, we noted that there is a prominent positive correlation between population density and PM_{2.5} concentration. That is, the higher the population density, the higher the PM_{2.5} concentration [60]. Taking Changsha–Zhuzhou–Xiangtan urban agglomeration as the study area, we found that the correlation between night-time light index and PM_{2.5} is not high (only 0.034 in 2009), but this correlation showed an

upward trend, reaching 0.135 in 2018. It can be seen from the results that the effect of different indexes on $PM_{2.5}$ concentration changed with the change in time and region. The dominant factors in spatial differentiation of $PM_{2.5}$ concentration are meteorological factors, natural conditions, and socio-economic status [61]. Our study shows that natural conditions are the dominant factor affecting $PM_{2.5}$ concentration, followed by meteorological factors, and, finally, social and economic conditions, in which leaf area index (LAI) has the strongest driving force on the spatial differentiation of $PM_{2.5}$ concentration [62]. As for the source of $PM_{2.5}$, previous studies have pointed out that the high concentration of $PM_{2.5}$ in the northwest of this urban agglomeration mainly comes from industrial emissions from thermal power, iron and steel, non-ferrous smelting, and cement industries. Sudden air pollution incidents are often related to straw burning [63]. Therefore, this urban agglomeration needs to speed up the pace of industrial transformation and upgrading, reduce the share of enterprises with high energy consumption and high pollution, and strengthen the management and control of straw burning and non-point source pollution in agricultural production [64]. Population density and the night light index reflect the degree of traffic exhaust to a certain extent. Under the condition of data limitation, based on the strong correlation among them, we used population density and night light index instead of traffic exhaust to study its impact on $PM_{2.5}$ concentration. In fact, traffic exhaust is an important source of $PM_{2.5}$ concentration. We will further study the mechanism by which traffic exhaust affects the change in $PM_{2.5}$ concentration and its centre of gravity in the future, with the help of these sources such as Waze, Google, or NOx.

Poor air quality not only seriously restricts the sustainable development of the social economy, but also threatens the health of people. Changsha–Zhuzhou–Xiangtan urban agglomeration is a key area for the prevention and control of air pollution in China. Since 2011, the joint prevention and control of air pollution in this region has achieved remarkable results, and the quality of air has been dramatically improved. Its achievements in building a resource-saving and environment-friendly society are undeniable [65]. However, it is worth noting that the decline rate of $PM_{2.5}$ concentration in the region has slowed significantly since 2016, possibly due to coal combustion, industrial pollution emissions, and motor vehicle exhaust emissions [39]. Furthermore, our study showed that the abnormal development trend of $PM_{2.5}$ concentration in some agricultural areas of this urban agglomeration is becoming more and more significant. The government needs to make more efforts to reach the goal of an annual average $PM_{2.5}$ concentration of less than $35 \mu\text{g}/\text{m}^3$ by 2025, which was set in the “Fourteenth Five-Year Plan for Ecological Environment Protection.”

5. Conclusions

This paper systematically analyses the spatial and temporal evolution characteristics and the future development trend of $PM_{2.5}$ concentration in Changsha–Zhuzhou–Xiangtan urban agglomeration from 2009 to 2018 by using the gravity model, spatial autocorrelation, Hurst index, and GIS spatial analysis methods. It also reveals the driving mechanism of the spatial differentiation of $PM_{2.5}$ concentration from the aspects of natural conditions, meteorological factors, and social and economic conditions.

The results of our study indicate that the concentration of $PM_{2.5}$ showed an inverted U-shaped trend from 2009 to 2018, rising from $62.26 \mu\text{g}/\text{m}^3$ in 2009 to $63.6 \mu\text{g}/\text{m}^3$ in 2011, and then decreasing to $41.4 \mu\text{g}/\text{m}^3$ in 2018. The spatial distribution of $PM_{2.5}$ concentration shows significant differences and aggregation. The high-value area is primarily scattered in the northwest region, with low elevation and a developed economy, while the low-value area is primarily scattered in the southeast region, with high altitude and an underdeveloped economy. From 2009 to 2018, the spatial centre of gravity of $PM_{2.5}$ concentration showed an overall trend of moving to the southeast. In addition, the concentration of $PM_{2.5}$ in most areas will continue the trend of gradual decline which has been seen the past, except in some rural areas of Chaling and Yanling counties. This may be due to the increase of $PM_{2.5}$ concentration caused by straw burning, waste incineration, mining, and large-scale project construction.

The geographical detection results regarding the spatial differentiation of PM_{2.5} concentration show that natural condition driving factors, as well as meteorological driving factors, have a significant influence on the spatial differentiation of PM_{2.5} concentration in this urban agglomeration, while the influence of socio-economic factors is small, but rapidly increasing.

Author Contributions: Conceptualization, Y.S. and Y.Z.; methodology, W.C. and Y.S.; software, W.C.; validation, C.D.; formal analysis, C.Z.; data curation, W.C.; writing—original draft preparation, W.C.; writing—review and editing, Y.S. and C.Z.; visualization, C.D.; supervision, Y.S.; funding acquisition, Y.S. and Y.Z. All authors have read and agreed to the published version of the manuscript.

Funding: This research was funded by Hunan Provincial Forest Quality and Efficiency Improvement Demonstration Project (OT-S-KTA6) under the Loan of the European Investment Bank; Forestry Department of Hunan Province: XLK202103-2; Central South University of Forestry and Technology: none.

Institutional Review Board Statement: Not applicable.

Conflicts of Interest: The authors declare no conflict of interest.

References

- Ding, Y.; Wu, P.; Liu, Y.; Song, Y. Environmental and Dynamic Conditions for the Occurrence of Persistent Haze Events in North China. *Engineering* **2017**, *3*, 266–271. [[CrossRef](#)]
- Yang, D.; Wang, X.; Xu, J.; Xu, C.; Lu, D.; Ye, C.; Wang, Z.; Bai, L. Quantifying the influence of natural and socioeconomic factors and their interactive impact on PM_{2.5} pollution in China. *Environ. Pollut.* **2018**, *241*, 475–483. [[CrossRef](#)]
- Zhang, N.; Huang, H.; Duan, X.; Zhao, J.; Su, B. Quantitative association analysis between PM_{2.5} concentration and factors on industry, energy, agriculture, and transportation. *Sci. Rep.* **2018**, *8*, 9461. [[CrossRef](#)] [[PubMed](#)]
- Hu, C.-G.; Lee, K.-H. Chemical Composition of Fine Particulate Matter in the Downtown Area of Jeju City. *J. Environ. Sci. Int.* **2018**, *27*, 597–610. [[CrossRef](#)]
- Park, S. COVID-19 (Coronavirus Disease 2019) Outbreaks and Their Relationship with Atmospheric Concentrations of PM₁₀ and PM_{2.5}: A Case Study for Daegu Metropolitan City. *J. Korean Geogr. Soc.* **2020**, *55*, 453465.
- Huang, Q.; Chen, G.; Xu, C.; Jiang, W.; Su, M. Spatial Variation of the Effect of Multidimensional Urbanization on PM_{2.5} Concentration in the Beijing-Tianjin-Hebei (BTH) Urban Agglomeration. *Int. J. Environ. Res. Public Health* **2021**, *18*, 12077. [[CrossRef](#)]
- Mi, Y.; Sun, K.; Li, L.; Lei, Y.; Wu, S.; Tang, W.; Wang, Y.; Yang, J. Spatiotemporal pattern analysis of PM_{2.5} and the driving factors in the middle Yellow River urban agglomerations. *J. Clean. Prod.* **2021**, *299*, 126904. [[CrossRef](#)]
- Yan, J.-W.; Tao, F.; Zhang, S.-Q.; Lin, S.; Zhou, T. Spatiotemporal Distribution Characteristics and Driving Forces of PM_{2.5} in Three Urban Agglomerations of the Yangtze River Economic Belt. *Int. J. Environ. Res. Public Health* **2021**, *18*, 2222. [[CrossRef](#)]
- Hu, W.; Zhao, T.; Bai, Y.; Kong, S.; Xiong, J.; Sun, X.; Yang, Q.; Gu, Y.; Lu, H. Importance of regional PM_{2.5} transport and precipitation washout in heavy air pollution in the Twain-Hu Basin over Central China: Observational analysis and WRF-Chem simulation. *Sci. Total Environ.* **2021**, *758*, 143710. [[CrossRef](#)]
- Liu, Y.; Shi, G.; Zhan, Y.; Zhou, L.; Yang, F. Characteristics of PM_{2.5} spatial distribution and influencing meteorological conditions in Sichuan Basin, southwestern China. *Atmos. Environ.* **2021**, *253*, 118364. [[CrossRef](#)]
- Thunis, P.; Clappier, A.; Beekmann, M.; Putaud, J.P.; Cuvelier, C.; Madrazo, J.; de Meij, A. Non-linear response of PM_{2.5} to changes in NO_x and NH₃ emissions in the Po basin (Italy): Consequences for air quality plans. *Atmos. Chem. Phys.* **2021**, *21*, 9309–9327. [[CrossRef](#)]
- Bai, K.; Ma, M.; Chang, N.-B.; Gao, W. Spatiotemporal trend analysis for fine particulate matter concentrations in China using high-resolution satellite-derived and ground-measured PM_{2.5} data. *J. Environ. Manag.* **2019**, *233*, 530–542. [[CrossRef](#)] [[PubMed](#)]
- Liu, X.; Hadiatullah, H.; Tai, P.; Xu, Y.; Zhang, X.; Schnelle-Kreis, J.; Schloter-Hai, B.; Zimmermann, R. Air pollution in Germany: Spatio-temporal variations and their driving factors based on continuous data from 2008 to 2018. *Environ. Pollut.* **2021**, *276*, 116732. [[CrossRef](#)] [[PubMed](#)]
- Zhou, L.; Zhou, C.; Yang, F.; Che, L.; Wang, B.; Sun, D. Spatio-temporal evolution and the influencing factors of PM_{2.5} in China between 2000 and 2015. *J. Geogr. Sci.* **2019**, *29*, 253–270. [[CrossRef](#)]
- Luna, M.A.G.; Luna, F.A.G.; Espinosa, J.F.M.; Cerón, L.C.B. Spatial and temporal assessment of particulate matter using AOD data from MODIS and surface measurements in the ambient air of Colombia. *Asian J. Atmos. Environ.* **2018**, *12*, 165–177. [[CrossRef](#)]
- Tiwari, S.; Chate, D.M.; Pragya, P.; Ali, K.; Bisht, D.S. Variations in Mass of the PM₁₀, PM_{2.5} and PM₁ during the Monsoon and the Winter at New Delhi. *Aerosol Air Qual. Res.* **2012**, *12*, 20–29.
- Wang, Y.; Duan, X.; Wang, L. Spatial-Temporal Evolution of PM_{2.5} Concentration and its Socioeconomic Influence Factors in Chinese Cities in 2014–2017. *Int. J. Environ. Res. Public Health* **2019**, *16*, 985. [[CrossRef](#)]

18. Wu, Q.; Guo, R.; Luo, J.; Chen, C. Spatiotemporal evolution and the driving factors of PM_{2.5} in Chinese urban agglomerations between 2000 and 2017. *Ecol. Indic.* **2021**, *125*, 107491. [CrossRef]
19. Xia, X.-S.; Wang, J.-H.; Song, W.-D.; Cheng, X.-F. Spatio-temporal Evolution of PM_{2.5} Concentration During 2000–2019 in China. *Huan Jing Ke Xue* **2020**, *41*, 4832–4843.
20. Yang, D.; Chen, Y.; Miao, C.; Liu, D. Spatiotemporal variation of PM_{2.5} concentrations and its relationship to urbanization in the Yangtze River delta region, China. *Atmos. Pollut. Res.* **2020**, *11*, 491–498. [CrossRef]
21. Ye, C.; Chen, R.; Chen, M.; Ye, X. A new framework of regional collaborative governance for PM_{2.5}. *Stoch. Environ. Res. Risk Assess.* **2019**, *33*, 1109–1116. [CrossRef]
22. Zou, Y.; Jin, C.; Su, Y.; Li, J.; Zhu, B. Water soluble and insoluble components of urban PM_{2.5} and their cytotoxic effects on epithelial cells (A549) in vitro. *Environ. Pollut.* **2016**, *212*, 627–635. [CrossRef] [PubMed]
23. Li, J.; Wang, N.; Wang, J.; Li, H. Spatiotemporal evolution of the remotely sensed global continental PM_{2.5} concentration from 2000–2014 based on Bayesian statistics. *Environ. Pollut.* **2018**, *238*, 471–481. [CrossRef] [PubMed]
24. Jin, Q.; Crippa, P.; Pryor, S. Spatial characteristics and temporal evolution of the relationship between PM_{2.5} and aerosol optical depth over the eastern USA during 2003–2017. *Atmos. Environ.* **2020**, *239*, 117718. [CrossRef]
25. Carmona, J.M.; Gupta, P.; Lozano-Garcia, D.F.; Vanoye, A.Y.; Yepez, F.D.; Mendoza, A. Spatial and Temporal Distribution of PM_{2.5} Pollution over Northeastern Mexico: Application of MERRA-2 Reanalysis Datasets. *Remote Sens.* **2020**, *12*, 2286. [CrossRef]
26. Casallas, A.; Castillo-Camacho, M.P.; Guevara-Luna, M.A.; González, Y.; Sanchez, E.; Belalcazar, L.C. Spatio-temporal analysis of PM_{2.5} and policies in Northwestern South America. *Sci. Total Environ.* **2022**, *852*, 158504. [CrossRef]
27. Lim, C.-H.; Park, D.-H. Spatial clustering of PM_{2.5} concentration and their characteristics in the Seoul Metropolitan Area for regional environmental planning. *J. Korean Soc. Environ. Restor. Technol.* **2022**, *25*, 41–55.
28. Yang, J.; Liu, P.; Song, H.; Miao, C.; Wang, F.; Xing, Y.; Wang, W.; Liu, X.; Zhao, M. Effects of Anthropogenic Emissions from Different Sectors on PM_{2.5} Concentrations in Chinese Cities. *Int. J. Environ. Res. Public Health* **2021**, *18*, 10869. [CrossRef]
29. Hao, Y.; Liu, Y.-M. The influential factors of urban PM_{2.5} concentrations in China: A spatial econometric analysis. *J. Clean. Prod.* **2016**, *112*, 1443–1453. [CrossRef]
30. Knibbs, L.D.; Van Donkelaar, A.; Martin, R.V.; Bechle, M.J.; Brauer, M.; Cohen, D.D.; Cowie, C.T.; Dirgawati, M.; Guo, Y.; Hanigan, I.C.; et al. Satellite-Based Land-Use Regression for Continental-Scale Long-Term Ambient PM_{2.5} Exposure Assessment in Australia. *Environ. Sci. Technol.* **2018**, *52*, 12445–12455. [CrossRef]
31. Zhai, L.; Li, S.; Zou, B.; Sang, H.; Fang, X.; Xu, S. An improved geographically weighted regression model for PM_{2.5} concentration estimation in large areas. *Atmos. Environ.* **2018**, *181*, 145–154. [CrossRef]
32. Zhou, Y.; Li, L.; Sun, R.; Gong, Z.; Bai, M.; Wei, G. Haze Influencing Factors: A Data Envelopment Analysis Approach. *Int. J. Environ. Res. Public Health* **2019**, *16*, 914. [CrossRef] [PubMed]
33. Li, S.; Zhai, L.; Zou, B.; Sang, H.; Fang, X. A Generalized Additive Model Combining Principal Component Analysis for PM_{2.5} Concentration Estimation. *ISPRS Int. J. Geo-Inf.* **2017**, *6*, 248. [CrossRef]
34. Huang, W.; Wang, H.; Zhao, H.; Wei, Y. Temporal-spatial characteristics and key influencing factors of PM_{2.5} concentrations in China based on Stirpat model and Kuznets curve. *Environ. Eng. Manag. J.* **2019**, *18*, 2587–2604. [CrossRef]
35. Singh, V.; Singh, S.; Biswal, A. Exceedances and trends of particulate matter (PM_{2.5}) in five Indian megacities. *Sci. Total Environ.* **2021**, *750*, 141461. [CrossRef]
36. Xia, S.; Liu, X.; Liu, Q.; Zhou, Y.; Yang, Y. Heterogeneity and the determinants of PM_{2.5} in the Yangtze River Economic Belt. *Sci. Rep.* **2022**, *12*, 4189. [CrossRef]
37. Londoño-Ciro, L.A.; Cañón-Barriga, J.E. Metodología para la caracterización espacio-temporal de PM_{2.5} en el área urbana de la ciudad de Medellín-Colombia. *Rev. EIA* **2018**, *15*, 113–132. [CrossRef]
38. Kim, E.; Bae, C.; Kim, B.-U.; Kim, H.C.; Kim, S. Evaluation of the Effectiveness of Emission Control Measures to Improve PM_{2.5} Concentration in South Korea. *J. Korean Soc. Atmos. Environ.* **2018**, *34*, 469–485. [CrossRef]
39. EEDH. Phased Achievements Have Been Made in the Analysis of PM_{2.5} Sources of Urban Ambient Air in Changsha, Zhuzhou and Xiangtan. 2014. Available online: https://sthjt.hunan.gov.cn/sthjt/xxgk/xwdt/zxdt/201402/t20140207_4638787.html (accessed on 29 October 2022).
40. Hammer, M.S.; Van Donkelaar, A.; Li, C.; Lyapustin, A.; Sayer, A.M.; Hsu, N.C.; Levy, R.C.; Garay, M.J.; Kalashnikova, O.V.; Kahn, R.A.; et al. Global Estimates and Long-Term Trends of Fine Particulate Matter Concentrations (1998–2018). *Environ. Sci. Technol.* **2020**, *54*, 7879–7890. [CrossRef]
41. Chen, Z.; Yu, B.; Yang, C.; Zhou, Y.; Yao, S.; Qian, X.; Wang, C.; Wu, B.; Wu, J. An extended time series (2000–2018) of global NPP-VIIRS-like nighttime light data from a cross-sensor calibration. *Earth Syst. Sci. Data* **2021**, *13*, 889–906. [CrossRef]
42. Yang, K.; He, J.; Tang, W.; Qin, J.; Cheng, C.C. On downward shortwave and longwave radiations over high altitude regions: Observation and modeling in the Tibetan Plateau. *Agric. For. Meteorol.* **2010**, *150*, 38–46. [CrossRef]
43. Wang, J.-F.; Zhang, T.-L.; Fu, B.-J. A measure of spatial stratified heterogeneity. *Ecol. Indic.* **2016**, *67*, 250–256. [CrossRef]
44. Zhang, N.-N.; Guan, Y.; Yu, L.; Ma, F.; Li, Y.-F. Spatio-temporal distribution and chemical composition of PM_{2.5} in Changsha, China. *J. Atmos. Chem.* **2020**, *77*, 1–16. [CrossRef]
45. Zhang, Y.; Jiang, W. Pollution characteristics and influencing factors of atmospheric particulate matter (PM_{2.5}) in Chang-Zhu-Tan area. *IOP Conf. Ser. Earth Environ. Sci.* **2018**, *108*, 042047. [CrossRef]

46. Zhu, M.; Yan, J.; Cheng, X.; Li, F. Investigating the spatiotemporal PM_{2.5} dynamic and socioeconomic driving forces in Beijing based on geographical weighted regression. *J. Nonlinear Convex Anal.* **2021**, *22*, 2331–2345.
47. EEDH. Notice of Hunan Provincial Environmental Protection Department on Printing and Distributing the 13th Five Year Environmental Protection Plan of Hunan Province. 2016. Available online: https://sthjt.hunan.gov.cn/sthjt/xxgk/ghcw/ghjh/zhgh/201609/t20160919_4662756.html (accessed on 29 August 2022).
48. EEDH. Letter on the Implementation of the Environmental Co Governance Plan for the Changsha Zhuzhou Xiangtan Urban Agglomeration (2010–2020). 2012. Available online: https://sthjt.hunan.gov.cn/sthjt/xxgk/ghcw/ghjh/zxgh/201206/t20120605_4662567.html (accessed on 29 October 2020).
49. EEDH. Notice on Printing and Distributing the “Fourteenth Five Year” Ecological Environment Protection Plan of Hunan Province. 2022. Available online: https://sthjt.hunan.gov.cn/sthjt/xxgk/ghcw/ghjh/zhgh/202207/t20220728_27569082.html (accessed on 29 October 2022).
50. CCPG. Jujube Town: Straw Burning is Prohibited, Publicizing “Volunteer Red”, Guarding “Ecological Green”. 2022. Available online: <https://www.chaling.gov.cn/c12925/20220516/i1859783.html> (accessed on 29 October 2022).
51. LMPG. Liuyang Has the Highest Air Quality Excellence Rate in Changsha. 2018. Available online: https://www.liuyang.gov.cn/lyszf/zfgzdt/zwdt/201801/t20180108_5109544.html (accessed on 29 October 2022).
52. Wang, X.; Li, T.; Ikhumhen, H.O.; Sá, R.M. Spatio-temporal variability and persistence of PM_{2.5} concentrations in China using trend analysis methods and Hurst exponent. *Atmos. Pollut. Res.* **2022**, *13*, 101274. [[CrossRef](#)]
53. Huang, C.; Liu, K.; Zhou, L. Spatio-temporal trends and influencing factors of PM_{2.5} concentrations in urban agglomerations in China between 2000 and 2016. *Environ. Sci. Pollut. Res.* **2021**, *28*, 10988–11000. [[CrossRef](#)] [[PubMed](#)]
54. Wang, T.; Song, H.; Wang, F.; Zhai, S.; Han, Z.; Wang, D.; Li, X.; Zhao, H.; Ma, R.; Zhang, G. Hysteretic effects of meteorological conditions and their interactions on particulate matter in Chinese cities. *J. Clean. Prod.* **2020**, *274*, 122926. [[CrossRef](#)]
55. Chen, P. Study on coordinated development of urban environment and economy based on cluster computing. *Clust. Comput.* **2019**, *22*, 6335–6343. [[CrossRef](#)]
56. Wang, J.; Ogawa, S. Effects of Meteorological Conditions on PM_{2.5} Concentrations in Nagasaki, Japan. *Int. J. Environ. Res. Public Health* **2015**, *12*, 9089–9101. [[CrossRef](#)]
57. Zhang, F.; Peng, H.; Sun, X.; Song, T. Influence of Tourism Economy on Air Quality—An Empirical Analysis Based on Panel Data of 102 Cities in China. *Int. J. Environ. Res. Public Health* **2022**, *19*, 4393. [[CrossRef](#)] [[PubMed](#)]
58. Tenaw, D.; Beyene, A.D. Environmental sustainability and economic development in sub-Saharan Africa: A modified EKC hypothesis. *Renew. Sustain. Energy Rev.* **2021**, *143*, 110897. [[CrossRef](#)]
59. Han, S.; Sun, B. Impact of Population Density on PM_{2.5} Concentrations: A Case Study in Shanghai, China. *Sustainability* **2019**, *11*, 1968. [[CrossRef](#)]
60. Zhao, X.; Zhou, W.; Han, L.; Locke, D. Spatiotemporal variation in PM_{2.5} concentrations and their relationship with socioeconomic factors in China’s major cities. *Environ. Int.* **2019**, *133*, 105145. [[CrossRef](#)] [[PubMed](#)]
61. Yun, G.; He, Y.; Jiang, Y.; Dou, P.; Dai, S. PM_{2.5} Spatiotemporal Evolution and Drivers in the Yangtze River Delta between 2005 and 2015. *Atmosphere* **2019**, *10*, 55. [[CrossRef](#)]
62. Liang, D.; Ma, C.; Wang, Y.-Q.; Wang, Y.-J.; Chen-Xi, Z. Quantifying PM_{2.5} capture capability of greening trees based on leaf factors analyzing. *Environ. Sci. Pollut. Res.* **2016**, *23*, 21176–21186. [[CrossRef](#)]
63. Xu, B.; You, X.; Zhou, Y.; Dai, C.; Liu, Z.; Huang, S.; Luo, D.; Peng, H. The study of emission inventory on anthropogenic air pollutants and source apportionment of PM_{2.5} in the Changzhutan Urban Agglomeration, China. *Atmosphere* **2020**, *11*, 739. [[CrossRef](#)]
64. Pei, T.; Gao, L.; Yang, C.; Xu, C.; Tian, Y.; Song, W. The Impact of FDI on Urban PM_{2.5} Pollution in China: The Mediating Effect of Industrial Structure Transformation. *Int. J. Environ. Res. Public Health* **2021**, *18*, 9107. [[CrossRef](#)]
65. EEDH. Environmental Quality in Hunan Province in the First Half of 2016. 2016. Available online: https://sthjt.hunan.gov.cn/sthjt/xxgk/zdly/hjjc/hjtj/201607/t20160722_4663842.html (accessed on 30 October 2022).